Continental Shelf Research 112 (2016) 92–103

Contents lists available at ScienceDirect

Continental Shelf Research

journal homepage: www.elsevier.com/locate/csr

Research papers

Seasonal variability in the continental shelf waters off southeastern Australia: Fact or fiction?

J.E. Wood [a,1], A. Schaeffer [a,*], M. Roughan [a,b], P.M. Tate [c]

[a] Coastal and Regional Oceanography Lab, the School of Mathematics and Statistics, University of New South Wales, Sydney, NSW, 2052, Australia
[b] Sydney Institute of Marine Science, Mosman, NSW 2088, Australia
[c] Sydney Water Corporations, Sydney, Australia

ARTICLE INFO

Article history:
Received 4 May 2015
Received in revised form
6 November 2015
Accepted 9 November 2015
Available online 11 November 2015

Keywords:
East Australian Current
Continental shelf processes
Coffs Harbour
Sydney
Seasonal cycle
Current meter moorings
Integrated Marine Observing System

ABSTRACT

Seasonality is an important timescale driving variability in the waters of many continental shelf regions globally. Along the east coast of Australia, it has been recognised that the East Australian Current (EAC), the Western boundary current (WBC) of the South Pacific gyre, warms and strengthens in the Austral summer. Thus it has been hypothesised that shelf currents also warm and strengthen (poleward) annually. However, the EACs highly dynamic nature results in large variations in the latitude of separation from the coast and eddy shedding. Until recently the lack of long term in-situ observations on the shelf has precluded a study into low frequency (seasonal) variability in shelf circulation. Using at least 3 years of moored *in situ* temperature and velocity observations we investigate low frequency variability in shelf waters at 2 cross-shelf locations (i) upstream and (ii) downstream of the typical EAC separation latitude. The local winds vary bi-modally upstream and tri-modally downstream varying with the passage of fronts, thus do not drive a seasonal response in the circulation. Harmonic analysis of the velocity and temperature fields shows that upstream of the separation zone, only 6% of the velocity variability occurs on the seasonal timescale, compared to 49% of the temperature variability. Cross shelf temperature gradients and vertical velocity shear increase in summer with an increase in poleward heat advection in the EAC. Downstream of the separation point the influence of episodic eddy encroachments precludes seasonality in the vertical structure of the flow despite an annual cycle in the stratification. The seasonal cycle in temperature moves out of phase with increasing depths, with maxima (minima) in March (September) at 30 m compared to maxima (minima) in May (November) at the bottom. This is expected to have a large influence on the timing of nutrient injection onto the shelf, and thus phytoplankton species composition and abundance.

1. Introduction

Seasonal changes have been shown to have large influences on the waters of continental shelf regions. Processes such as annual heating and cooling, freshwater input through seasonal changes in rainfall and seasonal wind regimes have been shown to cause changes in the circulation and hydrography on the shelf in coastal regions (Amorim et al., 2012; Davis et al., 2013; Rennie et al., 1999).

The continental shelf of southeastern Australia is generally narrow, dropping to a depth of 4000 m often within 25–100 km of the coast (See Fig. 1). It is flanked by the EAC (the WBC of the South Pacific sub-tropical gyre), which flows along the eastern coast of Australia. The EAC tends to hug the continental slope north of 30° S periodically encroaching on the shelf (Roughan and Middleton, 2004; Schaeffer et al., 2013, 2014a) and separating from the coast around 31–32°S (Cetina-Heredia et al., 2014). Downstream of the separation zone, both warm and cold core eddies are formed (Everett et al., 2012; Mata et al., 2006). These eddies dominate regional circulation patterns and encroach on the shelf, driving cross-shelf water mass exchanges on the continental shelf (Cresswell, 1994; McClean-Padman and Padman, 1991; Schaeffer et al., 2013, 2014a).

Studies have shown that the EAC has a seasonal cycle; being stronger in summer compared to winter (Godfrey et al., 1980; Hamon et al., 1975; Ridgway and Godfrey (1997). Whether or not this leads to seasonality in the shelf circulation adjacent to the EAC has not previously been examined. Ridgway and Godfrey (1997) found a seasonal pattern in the transport of the EAC between 25

* Corresponding author.
E-mail addresses: juwood@noc.ac.uk (J.E. Wood), a.schaeffer@unsw.edu.au (A. Schaeffer), mroughan@unsw.edu.au (M. Roughan), peter.tate@sydneywater.com.au (P.M. Tate).
[1] Present address: National Oceanography Centre Waterfront Campus, European Way, Southampton SO14 3ZH Hampshire United Kingdom.

http://dx.doi.org/10.1016/j.csr.2015.11.006

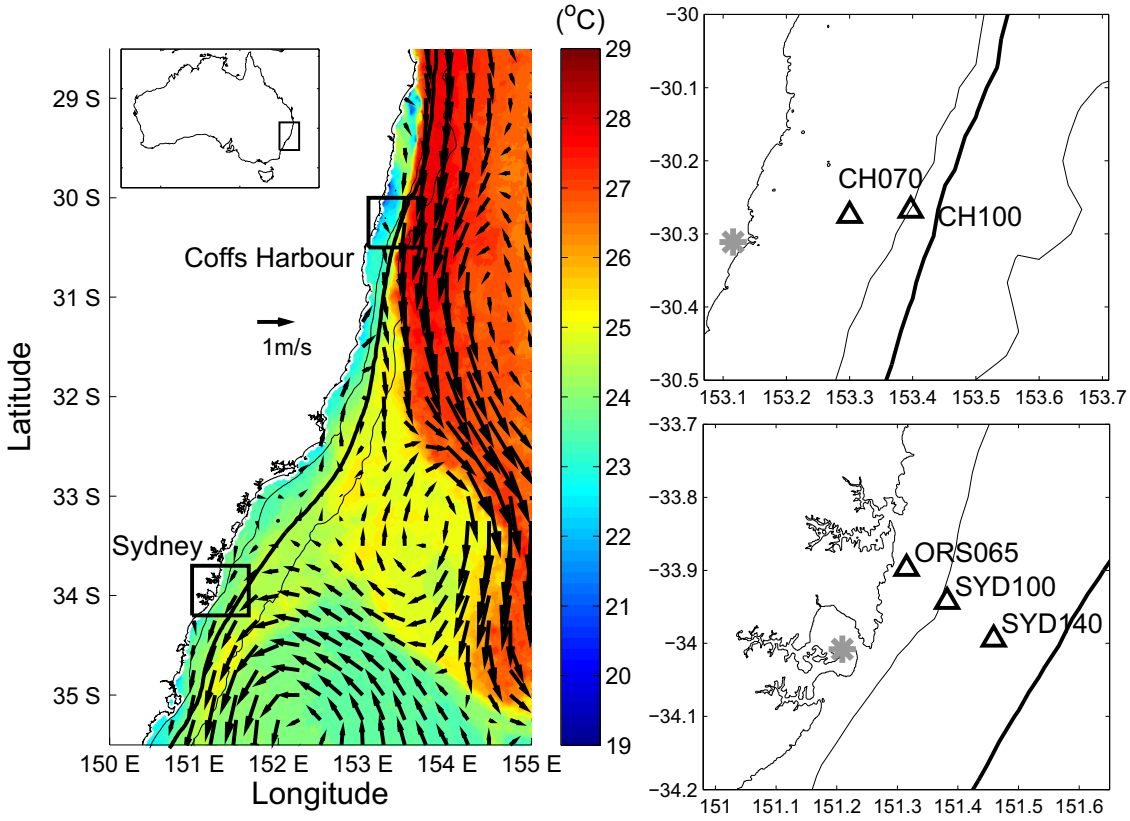

Fig. 1. Map of the study site. The black triangles indicate the location of the moorings measuring temperature and velocity. The grey stars show the location of the two wind stations. Super imposed on left panel is AVHRR L3S satellite sea surface temperature (colour) and velocity (arrows) from the 19th February 2010 (14 day composite) which shows the fast flowing warm EAC waters adjacent to Coffs Harbour and a large warm core eddy just south of Sydney. The coastline, 100 m, 200 m (bold) and 2000 m isobaths are also indicated.

to 45°S by investigating offshore steric heights derived from expendable bathythermograph data and historical hydrography. They used vertical profile observations of temperature and salinity to show that the EAC has a stronger poleward flow in the austral summer. They also showed that the EAC is broader in winter and then narrows in summer lying closer to the continental shelf with a strong return flow offshore (Ridgway and Godfrey, 1997).

Previous studies in this narrow (approximately 30 km wide) shelf region have shown faster poleward along-shelf currents on the continental shelf in summer compared with winter based on ship drift observations (inferring current velocities) between 25 and 38°S from 1854 to 1938 (data in the atlas Sea Areas Around Australia by the Nederlands Meteorologisch Instituut (1949) shown in Godfrey et al. (1980)). This was also confirmed by ship board currents taken upstream of the separation zone (27 to 32°S) at a mean distance offshore of 19 km over 18 months from in 1971 to 1973 (Hamon et al., 1975). However, recent work by Schaeffer et al. (2014b) used a 4 year time-series of moored observations at 5 min intervals in 65–140 m of water to show that EAC-driven bottom cross-shelf transport shows a quasi-periodical signal at a frequency of 90 (110) days upstream (downstream) respectively.

In terms of hydrography, seasonal variation on the continental shelf has previously been investigated by Malcolm et al. (2011) (upstream) and Hahn et al. (1977) (downstream) who both found a strong seasonal cycle in *in situ* temperatures. Downstream of the EAC separation zone, a suite of hydrographic parameters have been collected from two long term hydrographic stations located south of Sydney (Port Hacking) with seasonal and decadal processes identified in the temperature and biogeochemical fields (Hahn et al., 1977; Thompson et al., 2009).

Apart from the above mentioned studies, the waters of the continental shelf of southeastern Australia have been the subject of several short term (approximately one year or less) observational process studies (e.g., Church et al. (1986); Huyer et al. (1988); Griffin and Middleton (1991); Gibbs et al. (1998); Roughan and Middleton (2002, 2004)) or longer term studies using spatially limited hydrographic data (e.g., Newell (1966); McClean-Padman and Padman (1991); Thompson et al. (2009); Malcolm et al. (2011)). Many of the short term process studies were conducted during the austral spring and summer since it was expected that shelf currents are stronger in summer (Tranter et al., 1986). One example of the longest observational study, prior to 2008, was the Australian Coastal Experiment (Freeland et al., 1986). This 7 month experiment was designed to capture observations of coastal trapped waves with three mooring arrays collecting velocity data deployed at varying latitudes between September 1983 and March 1984 (Freeland et al., 1986). However a monthly breakdown of the data to determine seasonality was not undertaken. Furthermore, the point current meter moorings were deployed at the shelf-break (~140 m) and shelf slope (200 to 2000 m) rather than focusing on the continental shelf as is done here.

In 2008, the New South Wales node of the Australian Integrated Marine Observing System (IMOS) deployed two mooring arrays on the continental shelf of southeastern Australia upstream and downstream of the EAC separation zone. These mooring arrays provide an unprecedented dataset in temperature and current velocity, both upstream and downstream of the EAC separation zone. This dataset has brought new insight into the cross-shelf transport dynamics and the influence of the EAC in driving cold dense water uplift (Schaeffer et al., 2013, 2014a; Schaeffer et al.,

2014b). However, this is the first long term study of seasonal processes in the continental shelf waters of southeastern Australia. Considering the influence seasonality has on the coastal ocean properties more broadly, a more complete knowledge of this variability adjacent to a dynamic WBC is crucial.

This paper is organised as follows; the study site, observations and methods are described in Section 2 and Section 3 presents the results in terms of monthly climatology. Finally the results are discussed in Section 4 in the context of shelf regions adjacent to other WBCs.

2. Observations and methods

2.1. Datasets

NSW IMOS has deployed two mooring arrays upstream and downstream of the separation zone of the EAC (Fig. 1, (Roughan and Morris, 2011; Roughan et al., 2010; Roughan et al., 2015). Two moorings are located off the coast of Coffs Harbour (30°S) at the 70 m and 100 m isobaths (named CH070 and CH100 respectively), and three moorings are located off the coast of Sydney (34°S) on the 65 m, 100 m and 140 m isobaths (named ORS065, SYD100 and SYD140 respectively) (Table 1 and Fig. 1). These moorings are fully described in Schaeffer et al., (2013, 2014a) and Schaeffer et al., (2014b) and hence briefly described here. At each mooring, a bottom-mounted acoustic Doppler current profiler (ADCP) measures the current velocity in 4 m bins (8 m at SYD140) and thermistors measure temperature every 8 m (4 m at ORS065). Measurements were collected every 5 min and were quality controlled using the using the IMOS Toolbox version 2.1 (See http://code.google.com/p/imos-toolbox/) before being averaged to hourly.

Hourly wind speed (in km h^{-1} to one decimal place accuracy) and direction (to the nearest 10°) at nearby land-based sites (at 30°S, Coffs Harbour (CH-W); at 34°S Kurnell (KN-W), deemed appropriate by Wood et al. (2012), were provided by the Australian Bureau of Meteorology (Table 1). Wind stress was calculated as per Gill (1982).

As with most long-term data sets, there are a number of data gaps resulting from instrument loss or failure (Table 1), however in this case greater than at least 77% of the data for each parameter were returned. Data gaps of less than one day were filled using a modified linear interpolation as described in Wood et al. (2012). Due to the phased nature of the mooring deployments (Table 1, Fig. 2), upstream (downstream) of the separation zone three (four) years of current velocity and temperature data were used from 2010 to 2012 (2009–2012). Four years of wind data were used at both locations (2009–2012).

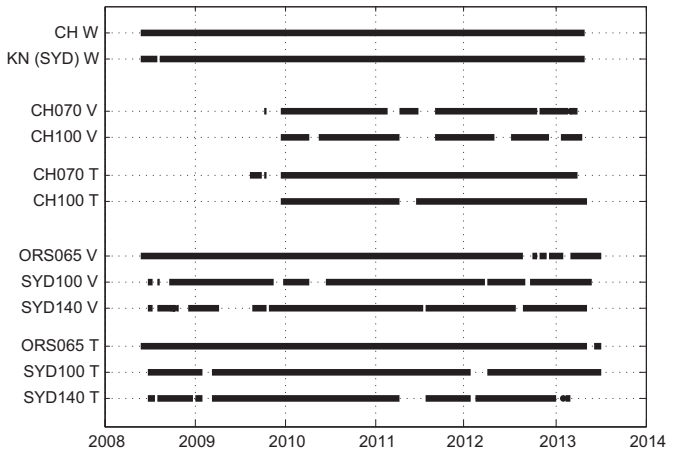

Fig. 2. Data availability for each wind site (CH -W and KN (SYD)-W) and each mooring (CH, ORS065, SYD), with T indicating temperature, V indicating current velocity and W indicating wind observations. For temperature, the data was considered available if more than half of the thermistor string returned observations.

Hourly wind stress, temperature and current velocities were low-passed filtered with a 38 h cut-off frequency with the ends cosine tapered (Beardsley et al., 1983). North/South and East/West wind stresses and current velocities were rotated according to their calculated principle axis (for currents the principle axis was calculated based on the depth-averaged currents for each mooring, Table 1).

2.2. Harmonic fitting

Low-passed filtered hourly temperature and along-shelf current velocities were sub-sampled every 2 days (this allowed more independence at each data point as the filter is 38 h, which is important for the significance test used). 6-hour subsampled data was also tested and did not show any considerable differences in the results. For the purposes of harmonic fitting, the same length of time (just over three years) was used for each time series (i.e., based on the shortest time series available for the parameters). As each parameter had a different number of missing data points, gaps were introduced so that the time series for each parameter (i.e., temperature and velocity) had the same number of data gaps. This is important for directly comparing the results from the fits of the harmonic regressions between different moorings.

The harmonic model used as per Lentz (2008), includes the annual harmonic,

Table 1
Description of the meteorological sites and oceanographic mooring sites. CH-W is Coffs Harbour wind, KN-W is Kurnell wind, ORS065 is the Ocean Reference Station, SYD is Sydney. The parameters (Para.) recorded at each site are wind (W), temperature (T) and current velocities (V). Start and End refer to the start date and end date for the time series of data available at the time of this study. Coverage (%) shows the percentage of data available between the Start and End date. Rotation refers to the orientation of the major axis (°) and is the rotation angle for the converting the North/South and East/West currents into along-shelf and across-shelf currents.

Site	Para.	Lat (°S)	Lon (°E)	Start	End	Coverage (%)	Rotation (°)
CH-W	W	30.311	153.119	01 June 2008	02 May 2013	100	21.4
KN-W	W	34.004	151.211	01 June 2008	02 May 2013	99	30.4
CH070	V	30.275	153.300	17 Dec 2009	03 Apr 2013	89	6.9
	T			15 Aug 2009	04 Apr 2013	95	
CH100	V	30.268	153.397	17 Dec 2009	21 Apr 2013	77	5.8
	T			16 Dec 2009	05 May 2013	94	
ORS065	V	33.898	151.315	01 June 2008	02 July 2013	96	15.4
	T			01 June 2008	03 July 2013	98	
SYD100	V	33.943	151.382	26 June 2008	29 May 2013	89	19.1
	T			25 June 2008	03 July 2013	95	
SYD140	V	33.994	151.459	26 June 2008	06 May 2013	86	30.1
	T			25 June 2008	06 Mar 2013	88	

$$A_t = A_0 + a\cos(\omega t) + b\cos(\omega t)$$

with calculation of the associated amplitude and phase of the annual cycle.

To determine the proportion of variability captured by the annual harmonic we calculated the variance explained by the harmonic using,

$$R^2 = 1 - \frac{RSS}{TSS}$$

Where R^2 is the square of the correlation coefficient, RSS is the residual sum of squares calculated as,

$$RSS = \sum_{t=1}^{n} (y_t - A_t)^2.$$

$y_t$is the observation for time t for the length (n) of the data series, and A_t is the value for the regression at that point in time. TSS is the total sum of squares calculated as,

$$TSS = \sum_{t=1}^{n} (y_t - \bar{y})^2$$

where $\bar{y}$ is the mean of y_t.

The significance of the fit was determined using a bootstrap method described by Strub et al. (1987) and briefly described here. The data for each variable were scrambled randomly 1000 times and re-fitted using the same regression formula. The significance of fit was determined based on the number of times the randomly scrambled data had amplitudes greater than the original time series i.e. , if there were 20 times when the amplitude was greater than the original time series, this corresponded to a 98% significance level. The fit was deemed significant if the significance level was greater than 80% as per Strub et al. (1987).

For temperature, the time of year of maximum heating was determined as being the time of year of the greatest change in the temperature fitted harmonic (i.e. steepest, positive gradient).

2.3. Calculation of vertical velocity shear

Seasonality in the along-shelf vertical velocity shear was investigated using monthly values of $\frac{dv}{dz}$ calculated from the *in situ* (ADCP) velocity measurements. The results were compared to the vertical along-shelf velocity shear derived from the thermal wind equation

$$\frac{dv}{dz} = -\frac{g}{\rho f}\frac{d\rho}{dx}$$

Where $\frac{dv}{dz}$ is the current shear (s^{-1}), g is the gravity acceleration (9.8 m s^{-2}), f is the Coriolis parameter (being -7.3591×10^{-5} s^{-1} at CH100 and -8.1522×10^{-5} s^{-1} at SYD140), $\frac{d\rho}{dx}$ is the cross shelf density gradient (kg m^{-4}) calculated every 8 m vertically through the water column.

The density ρ (kg m^{-3}) was calculated at each site according to methods provided under TEOS-10 (IOC 2010) with δS_A taken from version 3.0 of the McDougall et al., (2012) database.

While the moorings do not measure water column salinity, monthly hydrographic data were collected off CH (May 2011–Feb 2012, Armbrecht et al., (2015)) and off Port Hacking, 20 km south of SYD moorings (since 1944, Hahn et al., (1977) and Thompson et al. (2009)).

Surface salinity ranged between 35 to 35.6 at CH during the one year of sampling, while at Port Hacking, salinity appears to be slightly higher in winter compared to summer by approximately 0.4, fluctuating between 35.2 and 35.6.

We found that the thermal shear changed by a maximum of 0.25% when using the lower salinity value (35.2) compared to the upper salinity value (35.6) indicating that temperature is the main contributor to the density function in this area, as evidenced in Schaeffer et al., (2014b). Thus, given that we do not have a salinity time series that matches our temperature time series both spatially and temporally, we used a constant salinity of 35.4.

The density gradient was calculated between pairs of adjacent moorings (i.e. , CH070 with CH100, ORS065 with SYD140).

Finally a depth averaged velocity shear was calculated for the monthly values for $\frac{dv}{dz}$ from the ADCP observations and from the thermal wind equations.

3. Results

3.1. Monthly variability in wind stress

Upstream of the separation zone, the wind stress within each month tends to alternate between northward winds and southward winds (an example of a monthly wind rose for data from all Septembers during the study period is shown in Fig. 3). Downstream of the separation zone, the winds vary in three main directions, north-eastward, southward and eastward (Fig. 3). Therefore, super-imposed on the variance ellipses the monthly wind stress is averaged in the north and south directions upstream (Fig. 4), while downstream an average is presented for the three dominant directions (Fig. 5).

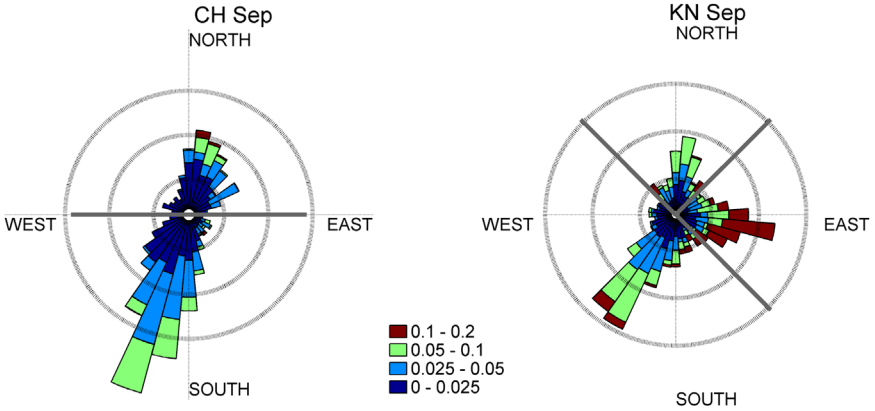

Fig. 3. Wind rose plots of wind speed and direction for September between 2009 and 2012 (aggregated) in Coffs Harbour station (CH, left panel) and Kurnell (Sydney) station (KN, right panel). Oceanographic convention is used (i.e., the direction to which the wind is going). The magnitude of the wind stress is indicated by the legend in N m^{-2}. Frequency at the 2% (inner dotted circle), 5% (middle dotted circle) and 8% (outer dotted circle) are shown. The solid grey lines indicate the calculated area for the quadrant means used in Figs. 4 and 5.

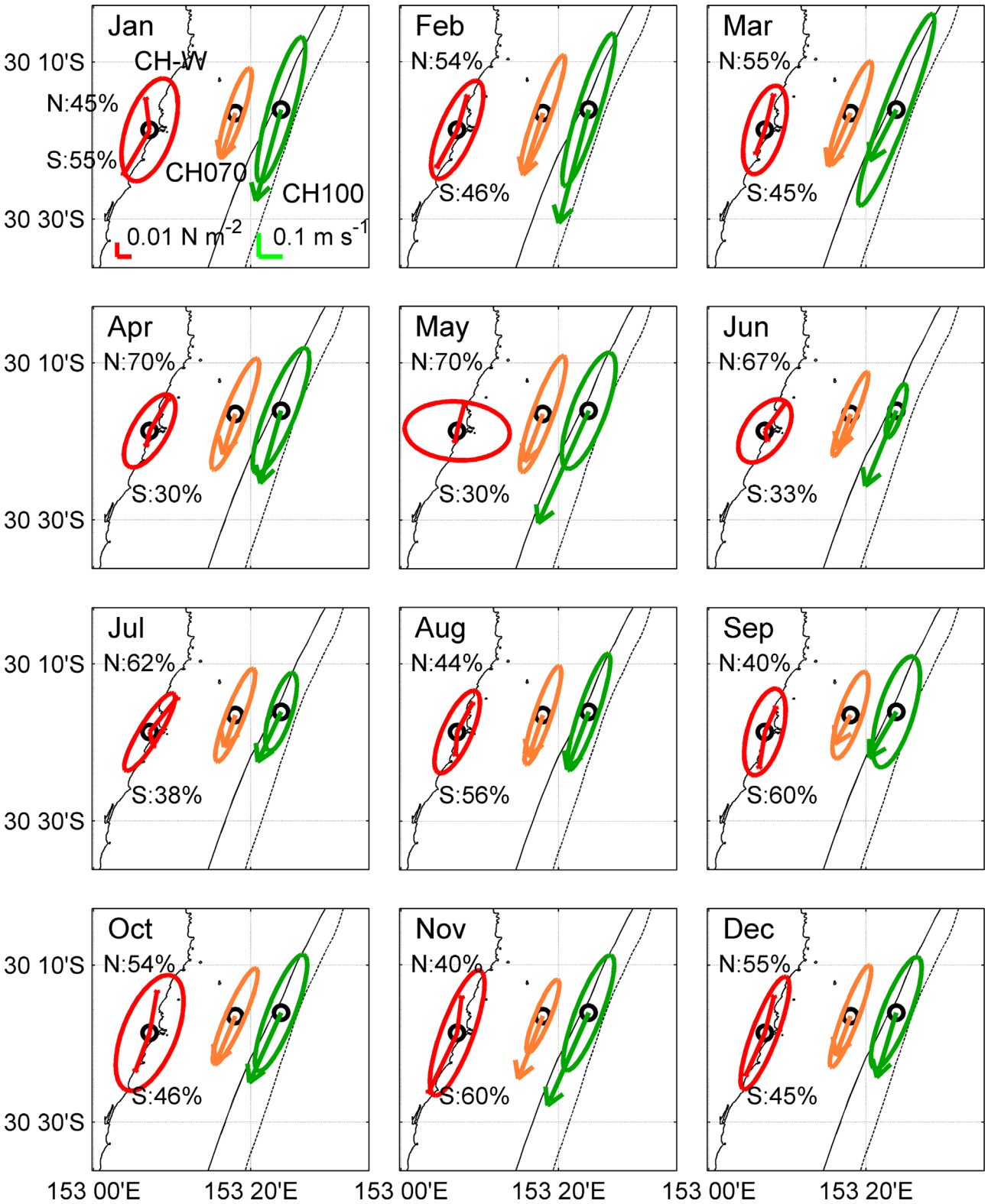

Fig. 4. Map showing mean depth-averaged current vectors and variance ellipses (CH070, orange, CH100, green) using hourly data over 2010 to 2012 for each month. Wind stress variance ellipses at CH-W (red) are presented using hourly data over 2009 to 2012. For wind stress, for each month the average for two quadrants are shown as in Fig. 3. The percentage text in the figure indicates how much of the time during that month that the wind stress was within that quadrant. The scale of the distance and legend of wind stress (red, N m^{-2}) and current velocity (green, m s^{-1}) shown on the top left plot are the same for all. The 100 m isobath (solid) and 200 m isobath (dashed) are also shown. (For interpretation of the references to color in this figure legend, the reader is referred to the web version of this article.)

At both latitudes, the variance ellipses for the wind stress tend to be isotropic, indicating there are large fluctuations in the wind direction and intensity. Upstream of the separation zone, August through to March (roughly the austral spring, summer and autumn) is generally characterised by both north-eastward winds and south-westward winds. Thus during each of these months

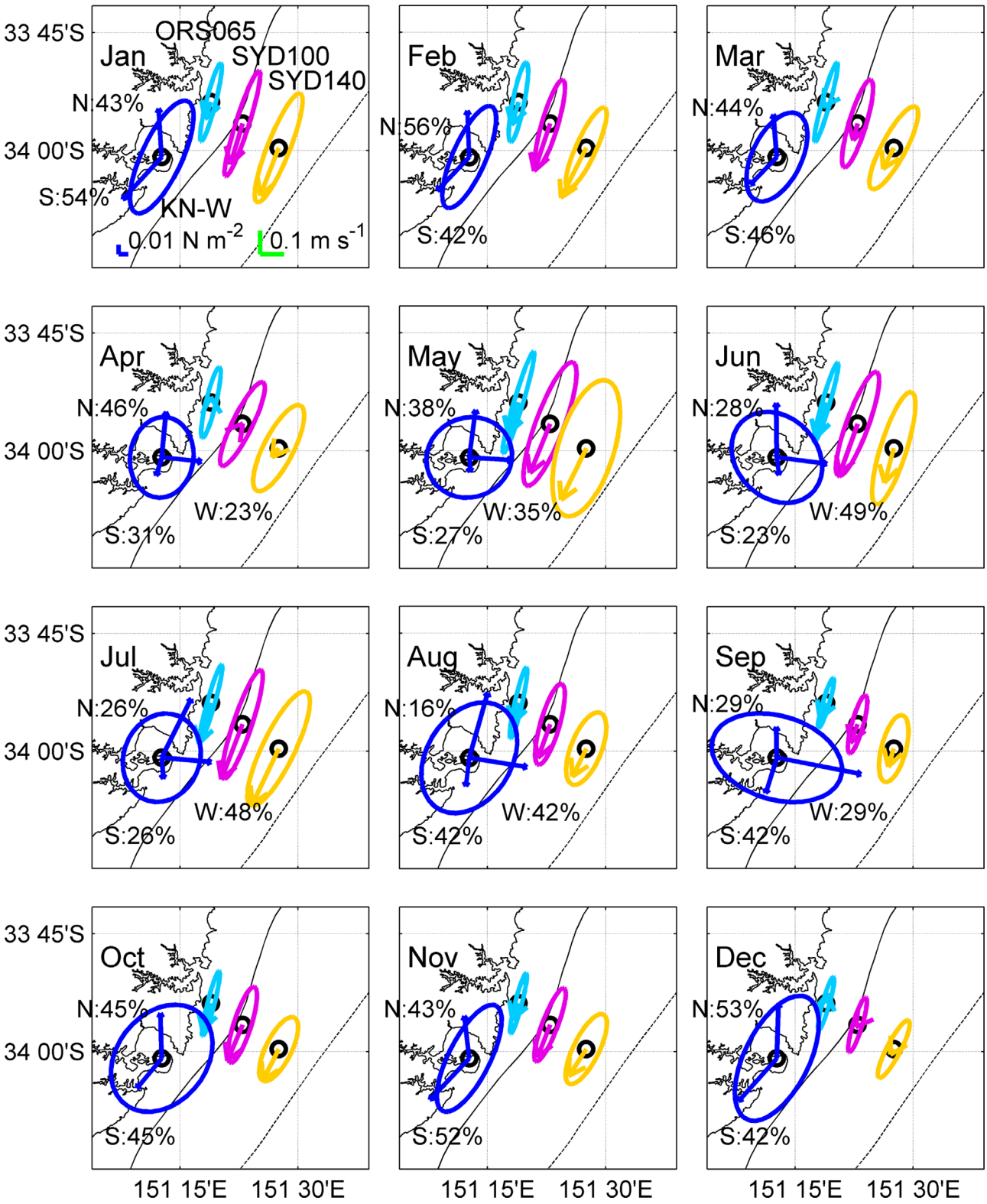

Fig. 5. Map showing mean depth-averaged current vectors and variance ellipses (ORS065, light blue, SYD100, pink, SYD140, yellow) and wind stress variance ellipses at KN-W (dark blue) using hourly data for 2009 to 2012 for each month. For wind stress, for each month the average for three quadrants are shown as indicated by Fig. 3. The percentage text in the figure indicates how much of the time during that month that the wind stress was within that quadrant. The mean in each quadrant is only shown if the wind was in that direction more than 10% of the time. The scale of the distance and legend of wind stress (dark blue, N m^{-2}) and current velocity (green, m s^{-1}) shown on the top left plot are the same for all. The 100 m isobath (solid) and 200 m isobath (dashed) are also shown. (For interpretation of the references to color in this figure legend, the reader is referred to the web version of this article.)

there were periods of both downwelling and upwelling favourable wind stress. These results are in good agreement with the findings of Rossi et al. (2014) based on remotely sensed sea surface winds, who showed that at this location, there is a mean of 7 to 10 days per month of upwelling favourable winds from August to February. In contrast, between April to July (roughly the austral autumn and

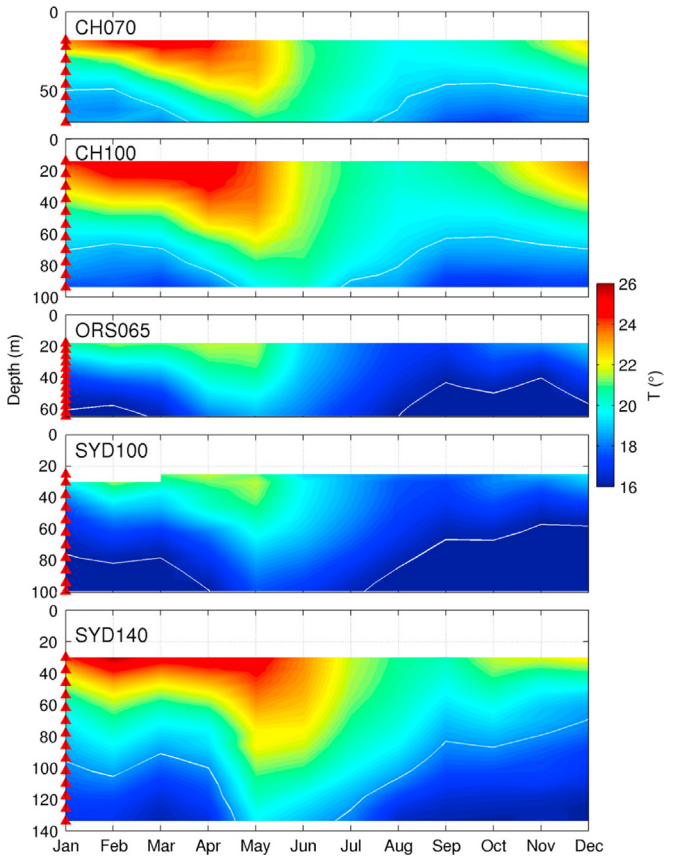

Fig. 6. Monthly mean temperature at each site. For CH moorings (CH070 and CH100) the 19 °C isotherm is shown (super-imposed in white). For SYD moorings (ORS065, SYD100 and SYD140), the 16 °C isotherm is shown (super-imposed in white). The temperature scale is the same for all plots and observation depths are indicated by red triangles.

winter) the wind is mostly north-eastward (downwelling favourable). Similarly, the austral summer downstream (October to March) is characterised by both north-eastward winds and southward winds. However, eastward (offshore) winds occur between April to September, in combination with either or both northward and south-westwards.

3.2. Monthly variability in along-shelf circulation

Upstream of the separation zone (CH), the mean depth-averaged current direction is poleward for all months, however the magnitude varies (Fig. 4). The strongest depth-averaged mean current magnitudes at CH100 are observed in January (0.40 m s^{-1}), February (0.50 m s^{-1}) and November (0.42 m s^{-1}). Although, during May the mean current magnitude was 0.52 m s^{-1}, however this month had very low data return, (see Fig. 2 CH100 C, where data gaps in 2011 and 2012 both included May). This is fairly consistent with the observations closer inshore at CH070. The weakest mean depth-averaged current magnitudes at both CH070 and CH100 were observed in July and September (0.23 m s^{-1} at CH100 and 0.14 m s^{-1} at CH070, for both months), suggesting that the mean depth-averaged current magnitudes are stronger in the austral summer than the austral winter. However, some of the other months do not fit with this pattern (e.g., December (August), austral summer (winter) has a mean depth-averaged magnitude of 0.29 (0.26) m s^{-1} at CH100 (CH070)). This indicates that the seasonal variability of the shelf circulation is more complex than the annual cycle in the EAC flow offshore.

The sub-monthly variability, indicated by the size and shape of the variance ellipses shows how representative the mean is of the current velocity for those months (i.e., narrow small ellipses imply small variability, thus the mean is quite representative of the time series, while large, broad ellipses indicate that the mean is not representative of the time series). For eight of the 12 months, the mean depth-averaged current velocity based on hourly observations at CH100 is larger than the major axis of the variance ellipse indicating that the currents are generally poleward. This shows that the mean is a good indicator of the current velocity for that month. The exception is March, which has the greatest eccentricity in the ellipse, due to the occurrence of equatorward currents ~14% of the time. The magnitude of these currents were also relatively strong, being > 0.40 m s^{-1} more than 6% of the time. These current reversals are more frequent inshore at CH070 for all months except November when comparing the mean to the variance ellipses.

In contrast to upstream, where for each month the mean depth-averaged current direction was always southward, downstream of the separation zone, some months have a mean depth-averaged current that is northward (Fig. 5) at ORS065, for instance in April (0.02 m s^{-1}) and December (0.02 m s^{-1}). At SYD140, the mean depth-averaged current is always southward. The strongest mean depth-averaged currents were observed in July (austral winter) at all locations across the shelf, with a maximum southward depth-averaged flow at the shelf-break (0.26 m s^{-1} at SYD140) and a minimum inshore (0.18 m s^{-1} at ORS065). During this month, July, the mean depth-averaged currents are of a similar size to the variance ellipses indicating less variability in the current direction compared to other months (where the mean speed is greater than the variance). This is also observed in February (excepting ORS065), June (excepting SYD140), October and November and thus southward currents were more frequent than northward currents (i.e., limited current reversals). The weakest monthly currents were observed in December at SYD140 (0.03 m s^{-1}, southward) and April (0.00 m s^{-1} at SYD100 where northward and southward current cancelled each other out).

Consequently, there is no clear seasonal pattern in the mean depth-averaged currents downstream of the separation zone. The variability found throughout the year is attributed to the encroachment of eddies onto the shelf (Schaeffer et al., 2014b). Both upstream and downstream of the separation zone, the dominant flow direction is along-shelf. The minor axis of the variance ellipses for the depth averaged current velocities are between 0.03 to 0.07 ms^{-1} showing that currents are not directly along-shelf and also have an across-shelf component.

3.3. Monthly variability in stratification and vertical flow structure

The seasonal temperature cycle is similar upstream and downstream of the separation zone (Fig. 6). Monthly mean temperature shows warm waters in the upper portion of the water column during the austral summer (December to February) and autumn (March to May) at each location. Cool bottom waters, developing during the late austral winter and spring (August to November), are maintained throughout the austral summer due to sporadic but strong upwelling favourable winds (Figs. 4 and 5) and EAC encroachments driving slope water uplift (Rossi et al., 2014; Schaeffer et al., 2014b). Thus stratification increases during the summer (December) to early autumn (April).

The decrease in the occurrence of upwelling favourable winds (and an increase in downwelling favourable winds) leads to a well-mixed water column during the winter. The result is that the bottom waters are actually warmer during the winter than summer, due to vertical mixing and the lack of upwelling-favourable winds during these months.

The vertical structure of the flow is generally dependent on the

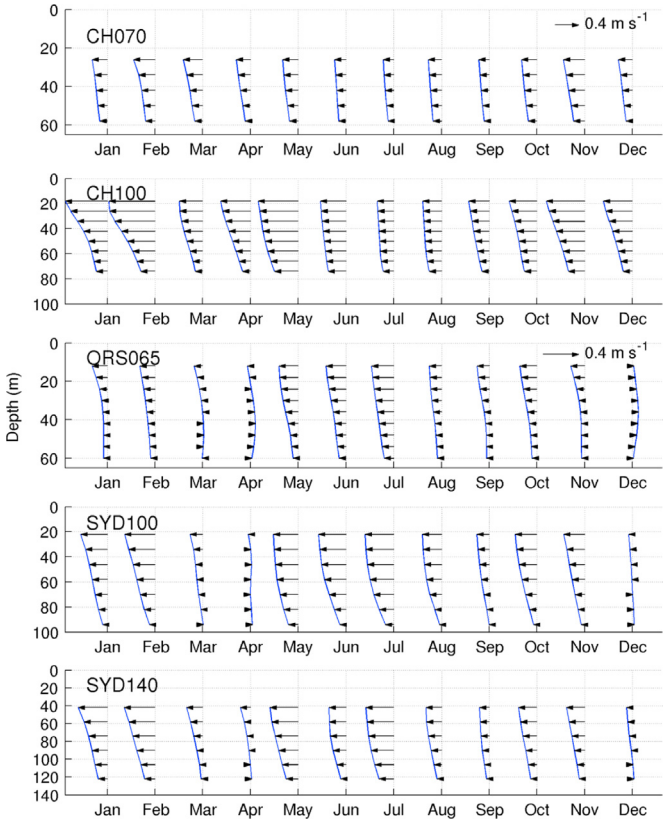

Fig. 7. Profile of monthly mean along-shelf current for each mooring. Arrows pointing to the left (right) indicate southward (northward) flow. The scaling for the profile of the currents upstream of the separation zone (CH070 and CH100, see legend in CH070) is different to that used for the profiles downstream of the separation zone (ORS065, SYD100 and SYD140, see legend in ORS065).

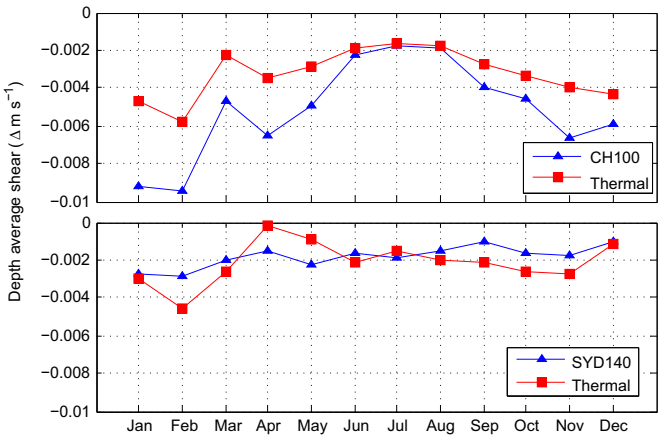

Fig. 8. Monthly mean depth-averaged vertical velocity shear computed from the ADCP observations at CH100 (top, blue) and SYD140 (bottom, blue). Also shown is the monthly mean depth-averaged along-shelf velocity shear calculated using temperature observations (and a constant salinity) between adjacent mooring pairs (CH070-CH100, top, red and ORS065-SYD140, bottom, red) using the thermal wind equation (see Section 2.3). (For interpretation of the references to color in this figure legend, the reader is referred to the web version of this article.)

stratification. A barotropic current is expected in winter when the water column is more homogeneous and a more baroclinic component of the flow in summer when the thermocline is more pronounced. Upstream, this seasonal cycle is followed, being more pronounced at CH100 (the shelf break) where the circulation is stronger (Fig. 7). In contrast, downstream, while the annual stratification profiles are similar to upstream there is no evidence of a robust seasonal cycle in the vertical structure of the flow (Fig. 7).

This was further investigated by comparing observed vertical velocity shear with the vertical velocity shear calculated from the temperature gradient (as described in Section 2.3, shown as a depth average in Fig. 8). Upstream of the separation zone, the results show a seasonal signal in the shear (Fig. 7), with strong shear in the mean along-shelf currents between November and May and only weak shear in June to October. This cycle is evident at both CH070 (data not shown) and CH100, however is stronger at the shelf-break (CH100).

Upstream of the separation zone the pattern of the buoyancy driven velocity shear (calculated using the thermal wind equation) follows that of the depth averaged vertical velocity shear being stronger in summer compared to winter (Fig. 8). Furthermore, while in winter the magnitude of the vertical shear is explained by the temperature driven flow, during summer the temperature driven shear only partially explains the stronger vertical current shear.

At 34°S, the depth-average buoyancy in continental shelf waters does not show any strong seasonality (Fig. 8, downstream). This indicates that the cross-shelf temperature gradient is more uniform seasonally downstream of the separation zone (in the absence of the warm EAC waters).

4. Quantifying the seasonality

The fitting of an annual harmonic to the temperature and along-shelf velocity data is a useful method for quantifying the variability explained by the seasonal cycle as demonstrated by Strub et al. (1987), Butman and Beardsley (1987) and Lentz (2008).

4.1. Temperature

As shown in Fig. 6, the ocean temperature exhibits a significant seasonal cycle (Table 2). At 30 m depth, the peak in the temperature cycle occurs at approximately the same time of year at both locations and across the shelf (during March, the end of summer). This is also the case for the time of year of maximum heating.

The percentage of variability explained is higher downstream than upstream, with 58–66% and 49% of the 30 m depth signal explained by the annual harmonic fit, respectively. Upstream of the separation zone, with only 49% of the temperature variability accounted for by the annual cycle (of which seasonal radiation is expected to be the major source), this means that half of the variability in the temperature cycle is driven by other factors. A contributor to this variability is likely to be the quasi-periodic EAC intrusions on the shelf (Schaeffer et al., 2014b). At CH100, in the near bottom, only 21% of the temperature variability is explained by seasonality (i.e., the annual cycle). This is consistent with the research by Schaeffer et al., (2014b) showing that episodic cold slope water intrusions are a typical feature both upstream and downstream of the separation zone and are dominated by a 90–100 day periodicity rather than the annual cycle.

Downstream, seasonality explains 44–51% of the bottom temperature variability (more than double that of upstream). Overall, the temperature harmonics show warmest water in March at 30 m, and in May close to the bottom. The greatest change in phase happens over depths at CH100, with a lag of 2.5 months between the temperature peaks. Amplitudes at 30 m are similar at all sites (~2 °C), decreasing at depth to 0.9–1.6 °C.

4.2. Velocity fields

Annual harmonic fitting for the along-shelf velocity is mostly

Table 2
Statistics of fit for the annual harmonic for temperature and along-shelf velocity. Two depths are shown, one in the upper half of the water column and the other near the bottom. For temperature (along-shelf velocity), the amplitude is in °C (m s^{-1}). For temperature, the date where the maximum temperature occurred is shown (Date of max. temperature) and the date of the maximum heating (Date of max. heating). For along-shelf velocity, the date where the maximum southward along-shelf velocity occurred is shown (Date of max. southward velocity, i.e., the time of year with the strongest southward velocity). Percentage explained (% explained) is how much of the variability is explained by the harmonic. NS means that the fit for that depth was not significant.

		Depth (m)	Amplitude (°C)	Date of max. temperature	Date of max. heating	% explained
Temperature	CH070	30	1.9	7 Apr	4 Jan	49
		62	1.4	27 May	23 Feb	34
	CH100	30	2.0	20 Mar	18 Dec	49
		94	1.4	7 Jun	6 Mar	21
	ORS065	30	2.1	9 Apr	6 Jan	58
		62	1.6	19 May	16 Feb	51
	SYD100	30	2.2	30 Mar	28 Dec	66
		94	1.2	25 May	22 Feb	44
	SYD140	30	2.2	24 Mar	23 Dec	66
		134	0.9	25 May	21 Feb	16
		Depth (m)	Amplitude (m s^{-1})	Date of max. southward velocity		% explained
Along-shelf current	CH070	26	0.04	31 Dec		1
		58	NS	NS		NS
	CH100	26	0.15	24 Jan		6
		74	NS	NS		NS
	ORS065	26	0.04	4 Aug		2
		58	0.01	16 Sep		1
	SYD100	26	NS	NS		NS
		74	NS	NS		NS
	SYD140	42	0.08	4 Feb		3
		122	NS	NS		NS

significant in shallow water (<42 m deep, except for SYD100), explaining only 1–6% of the signal variability (Table 2). The highest amplitude is at CH100 with 0.15 m s^{-1} and a maximum southward flow in January. At other locations, seasonality is barely significant, with amplitudes $<=0.08$ m s^{-1}, explaining $<=3$% of the variability. Interestingly, even though seasonality in velocity is barely present, the timing of the greatest southward flow differs, being consistently in summer upstream (Dec–Jan), in agreement with the most intense offshore EAC, and variable downstream (Table 2).

5. Discussion

5.1. Investigating seasonality

Robust seasonality was easily identified in the temperature of the waters on the continental shelf of southeastern Australia. The cycle of interior temperatures warming and cooling is consistent with expected seasonality (i.e. summer time heating and winter cooling). Peak heating at 30 m depth (18 Dec–6 Jan) occurs around the summer solstice, ~21 December, which is similar to that found in the English Channel by Bowers and Simpson (1990) for depths greater than 80 m. Close to the bottom, maximum heating occurs almost two months later (16 Feb–6 Mar).

Both upstream and downstream, the weakest seasonality in temperature was found in bottom waters and at the outer shelf. This is consistent with the impact of the cross shelf transport of slope bottom water, which has been shown to be mostly non-seasonal and dominated by a 90–100 day periodicity, in agreement with the frequency of EAC instabilities and eddy shedding (Schaeffer et al., 2014b, Mata et al., 2006).

Along the southern flank of Georges Bank upstream of the Gulf Stream separation zone seasonality is a much more important driver of temperature variability (90% at 45 m and 84% at 75 m) than off southeastern Australia (<66%). There are likely three reasons for this, the first being methodological – i.e., Butman and Beardsley (1987) used monthly averages (whereas we used a data point every 2 days) which decreases the influence of intra-monthly variability on the calculation of the percentage of variability explained by the seasonal cycle. Secondly, they used both an annual and semi-annual harmonic. This is useful as it does highlight the asymmetry in the temperature seasonal cycle, however we found that the addition of a semi-annual harmonic increases the variability explained by the model by only a few percentage. For example at CH070 at 30 m depth, where the greatest change was observed, the increase in the percentage of variability explained by the model with both the annual and semi-annual harmonic was only 9% (data not shown).

Finally, over the four year period used by Butman and Beardsley (1987), one eddy was identified to have encroached on the bank. On the southeastern coast of Australia, encroachment of both the EAC upstream and its eddies downstream on the continental shelf occurs more frequently. Schaeffer et al. (2014b) showed that encroachment upstream occurs with a periodicity of 90 days, while downstream, it occurs at 100 days indicating there is an encroachment event approximately three times per year. This would thus reduce the variability explained by the seasonal cycle here compared to the southern flank of Georges Bank, considering the impact of eddies on the temperature field.

In contrast to temperature, it was much more difficult to identify a seasonal cycle in the circulation. Weak seasonality was identified in the along-shelf velocities upstream of the separation zone (explaining 6% of the variability), however no clear seasonality was found downstream, in fact half of the results were found to be statistically insignificant (Table 2).

Butman and Beardsley (1987) found that 35% of the velocity variability was explained by the seasonal cycle at 45 m depth at the 85 m isobath. This is much higher than our findings and shows that the seasonal timescale is much more important in the waters of the continental shelf of eastern United States compared to the southeastern Australian continental shelf.

5.2. Drivers of seasonal circulation

5.2.1. Local wind forcing

Local wind stress has been shown to be an important driver of seasonal shelf circulation on many other continental shelves (e.g., in the South Atlantic Bight (Blanton et al., 2003), the West Florida Shelf (Liu and Weisberg, 2012) and the Mid-Atlantic Bight (Lentz, 2008, Kohut, et al., 2004, Gong et al., 2010)).

Liu and Weisberg (2012) showed that wind stress forcing was important in driving both the along-shelf and across-shelf current (through upwelling and downwelling) on the West Florida continental shelf. The West Florida Shelf is both wider and shallower than the southeastern Australian continental shelf. Current velocities most affected by the seasonal wind stress patterns were in water depths of 25 to 30 m.

Furthermore, the direction of the dominant wind stress over the West Florida shelf was seasonally consistent and thus drove a steady seasonal response in the circulation. In contrast, a strongly reversing bimodal wind pattern is observed on the southeastern Australian continental shelf throughout the year. Even during an upwelling favoured month, there are only approximately 10 days of upwelling favourable winds (Rossi et al., 2014), ie less than 30% of the time.

Therefore, the variability in the wind regime in this region precludes the evolution of a persistent seasonal wind driven circulation. This is confirmed by an absence of current veering with depth in the monthly averaged data (not shown) that is detected in the velocities on other continental shelves that see a more consistent wind stress (Liu and Weisberg, 2012).

Liu and Weisberg (2012) also found it was difficult to discern a seasonal pattern at deeper observation locations on the shelf from the 50 m isobath while the locations near the shelf break did not show any seasonality. The results found by Liu and Weisberg (2012) further offshore are consistent with the results presented here (i.e., a weak or in-discernible seasonal pattern). On the West Florida Shelf, Liu and Weisberg (2012) suggested that this is due to the proximity of the Loop Current and its eddies overwhelming the seasonal wind pattern at the shelf break.

Studies on the Mid Atlantic Bight have reported strong relationships between wind stress and current velocities as indicated by high correlations between the two. Using depth-averaged current velocities from ADCPs, similar to our study, Lentz (2008) found high correlations (0.8) with along-shelf wind stress in the Mid Atlantic Bight. He was thus able to derive a seasonal component of the along-shelf current velocity that was due to the wind stress. Kohut et al. (2004) also found high correlation (0.82) between HF radar surface current velocities and local wind stress using one year of data on the New Jersey Shelf (in the Mid Atlantic Bight).

Another study on the New Jersey Shelf, in similar depths as our study (offshore of the 60 m isobath), Gong et al., (2010), presented monthly correlations between across-shelf wind stress and along-shelf (across-shelf) current velocities greater than 0.8 (0.7) in summer (winter). These high correlations showed the importance of across-shelf wind stress as a driver of the shelf circulation, as opposed to along-shelf wind stress. Indeed, monthly correlations offshore of the 60 m isobath between along-shelf wind stress and current velocities were less than 0.6 (as low as 0.3 in summer time).

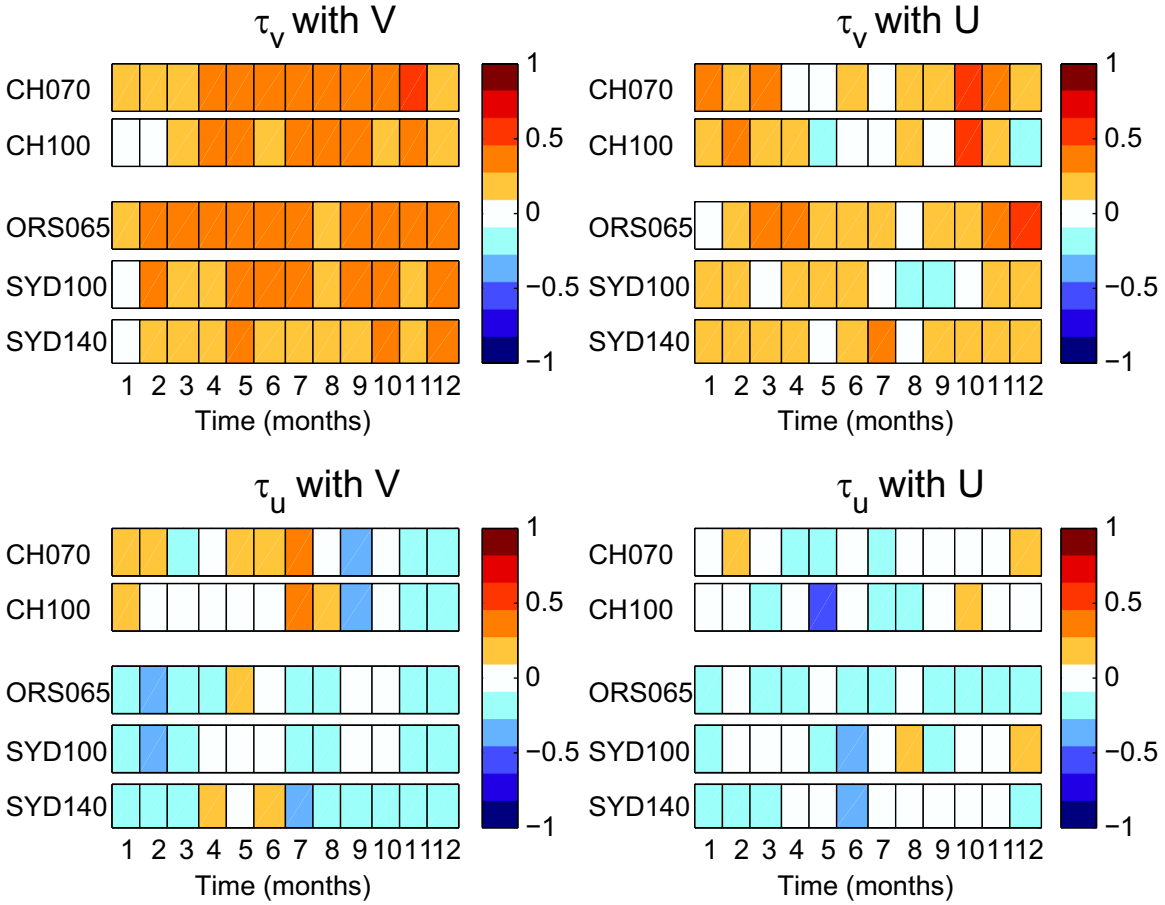

Fig. 9. Monthly correlation coefficients between along-shelf wind stress with depth averaged along-shelf velocity (top, left), along-shelf wind stress with depth averaged across-shelf velocity (top, right), across-shelf wind stress with depth averaged along-shelf velocity (bottom, left) and across-shelf wind stress with depth averaged across-shelf velocity for each site (bottom, right).

On the continental shelf of south eastern Australia, we found monthly correlations between the across-shelf wind stress and both the along and across-shelf current velocities of between −0.46 and 0.33 with an absence of seasonality (Fig. 9). This suggests that, contrary to the results for the Mid Atlantic Bight, here, across-shelf wind stress is not an important driver of shelf circulation. Furthermore, monthly correlations between along-shelf wind stress and along-shelf current velocities were less than 0.5 and also showed no seasonality indicating that along-shelf wind stress is not an important driver of circulation on the seasonal timescale.

The studies by both Kohut et al. (2004) and Gong et al. (2010) both used surface current velocities from HF radar, while our study correlated wind stress with depth-averaged current velocities and thus one would expect these correlations to be lower. However Mantovanelli et al. (in review) also found relatively low cross-covariance coefficients (less than 0.6) off Coffs Harbour between along-shelf wind stress and residual current velocity at the surface measured by HF radar.

5.2.2. Seasonal buoyancy forcing

Inter-annual variability in freshwater discharge from rivers has been shown to be a driver of seasonal density driven circulation. Li et al. (2014) showed that inter-annual variability in freshwater discharge from rivers in the Gulf of Maine considerably influences the hydrography and along-shelf current velocities on the shelf. Lentz (2008) attributed part of the annual cycle in the along-shelf currents in the Mid Atlantic Bight to the changing buoyancy driven by seasonal changes in freshwater input.

Along the coast of SE Australia, freshwater is typically low due to Australia being a generally arid nation. Dai and Trenberth (2002) showed that the freshwater discharge is between 1.9 to 12 $m^3 s^{-1}$ along the coast of SE Australia (depending on the calculation method) compared to between 113 to 128 $m^3 s^{-1}$ along the coast of the eastern United States.

Monthly mean surface salinity in waters off Sydney (at Port Hacking, approximately 20 km south of the SYD mooring line) was shown to vary by less than 0.4 throughout the year (Thompson et al., 2009) at the 100 m isobath. In comparison, salinity in the Mid-Atlantic Bight can vary by up to 1.5 throughout out the year (Lentz, 2008). Thus freshwater discharge is excluded as a seasonal buoyancy forcing mechanism in this region.

Seasonal temperature forcing does however provide an important contribution to along-shelf current seasonality upstream of the EAC separation zone. Here we show that the temperature gradient across the shelf drives a vertical shear in the along-shelf velocity that is stronger in summer than winter. However, we did not find any seasonality in the along-shelf currents, and EAC encroachment on the shelf has been shown to occur typically at a 90–100 day frequency (Schaeffer et al., (2014b). Therefore, we suggest that the seasonality we find in the velocity shear and the cross-shelf temperature gradient is simply due to an enhanced temperature difference between shelf and EAC waters in summer compared to winter, as shown in Schaeffer et al. (2013; 2014a). In addition we show that while in winter the magnitude of the vertical shear is explained by the temperature driven flow, during summer the temperature driven shear only partially explains the stronger vertical current shear, suggesting a potential influence of salinity gradients.

Unfortunately, there is only limited salinity data available at CH so it is difficult to conclusively assess the salinity gradient across the shelf. Evaporation and precipitation are expected to exhibit a significant seasonality in this sub-tropical region characterised by warm, wet summers and cool to mild dry winters (www.bom.gov.au). This could potentially increase the density gradient across the shelf during summer and thus explain the additional vertical shear above that shown to be caused by the temperature gradient.

5.3. Proximity to the shelf break

The continental shelf of southeastern Australia is narrow and relatively deep in comparison to the West Florida shelf and the Mid Atlantic Bight (e.g., the 65 m isobath is within 2 km of the coast off Sydney, compared to approximately 200 km from the coast on the West Florida shelf). Thus it appears that the proximity of the shelf break to the coast results in the EAC and its eddy field having a strong influence on the along-shelf coastal currents.

In this regard, the circulation over the width of the continental shelf in this region responds to forcing from the EAC and its eddy field in a similar way as the “shelf break” region at the edge of the South Atlantic Bight, influenced by the Gulf Stream (Blanton et al., 2003), or on the West Florida Shelf, influenced by the Loop current (Liu and Weisberg, 2012).

5.4. Implications for biological productivity

Using remote sensed observations of ocean colour, Everett et al. (2014) showed a marked difference in the chlorophyll-a dynamics between upstream and downstream of the separation zone. They showed that upstream of the separation zone a combination of wind forcing plus EAC encroachment resulted in the highest surface chlorophyll concentrations whereas downstream from our study site (35.5–38°S) concentrations were highest during the spring bloom.

In addition, during summer and autumn they observed the lowest surface chlorophyll concentrations despite our results showing coldest bottom temperatures, suggesting cross-shelf nutrient input. This is potentially due to the increase in stratification we observed during these months (Fig. 6), likely restricting the cholorophyll-a maximum to beneath the thermocline.

Recent work by Armbrecht et al. (2015) investigated the relationship between phytoplankton abundance and water-types at our upstream study site (30°S). Using 11 months of data they showed a seasonal increase in phytoplankton abundance for species that typically bloom in spring, however they also found lowest seasonality in the abundance of phytoplankton that prefer deeper cold saline watermasses. Our results support these findings showing that only 21% of the variability in the bottom waters offshore (particularly upstream, CH100) can be attributed to seasonality. Both these results are consistent with episodic cold slope water intrusions driven by the encroachment of the EAC (Schaeffer et al. 2014b) rather than a seasonal cycle of warming and cooling.

6. Conclusions

Along the coast of southeastern Australia, temperature shows a robust seasonal cycle, with the maximum bottom temperature occurring during winter (out of phase with the maximum in the interior water temperature cycle which occurs in summer) due to a well-mixed water column. We found an important difference upstream versus downstream of the EAC separation zone with the EAC causing a stronger cross-shelf temperature gradient driving a stronger vertical along-shelf velocity shear in summer compared to winter. In the absence of the EAC (downstream), this seasonal velocity shear was not detected. Unlike the waters on other continental shelves which are forced on the seasonal timescale, seasonality plays only a minor role in the circulation on the continental shelf of southeastern Australia. As little as 6% of the variability in the along-shelf velocities is explained by the seasonal cycle upstream of the separation zone. Many unique features about this continental shelf region, such as a narrow continental

shelf, a lack of consistent seasonal wind forcing, and an absence of any significant seasonal fresh water signal, results in the dominant forcing mechanisms being the quasi-periodic EAC encroachments and eddy shedding and the interaction with synoptic wind forcing. Contrary to popular belief, this combination results in a limited response in the circulation on the shelf at the seasonal timescale at Coffs Harbour (30°S) and Sydney (34°S). We expect that these non-seasonal forcing mechanisms will influence the timing of nutrient injection onto the shelf and the composition and abundance of phytoplankton blooms.

Acknowledgements

We are grateful for the support of our partners New South Wales (NSW) Office of Environment and Heritage, Oceanographic Field Services, Connell Wagner Consulting, Manly Hydraulics Laboratory, and Sydney Water Corporation. We appreciate the efforts of the NSW-IMOS moorings team in collecting the data used here. The Integrated Marine Observing System is supported by the Australian Government through the National Collaborative Research Infrastructure Strategy and the Super Science Initiative. Data from the ocean reference station (ORS065) were provided by Sydney Water Corporation. We also appreciate the constructive comments provided by two anonymous reviewers which improved this manuscript.

References

Amorim, F.N., Cirano, M., Soares, I.D., Campos, E.J.D., Middleton, J.F., 2012. The influence of large-scale circulation, transient and local processes on the seasonal circulation of the Eastern Brazilian Shelf, 13°S. Cont. Shelf Res. 32, 47–61.
Armbrecht, L.H., Schaeffer, A., Roughan, M., Armand, L.K., 2015. Interactions between seasonality and oceanic forcing drive the phytoplankton variability in the tropical-temperate transition zone (~30°S) of Eastern Australia. J. Mar. Syst. 144, 92–106.
Beardsley, R.C., Limeburner, R., Rosenfeld, L.K., 1983. Introduction to the CODE-2 Moored Array and Large-Scale Data Report WHOI Technical Report 85-35. In: Limeburner, R. (Ed.), Woods Hole Oceanographic Institution, pp. 1–242.
Blanton, B.O., Aretxabaleta, A., Werner, F.E., Seim, H.E., 2003. Monthly climatology of the continental shelf waters of the South Atlantic Bight. J. Geophys. Res.: Ocean. 108, 3264.
Bowers, D.G., Simpson, J.H., 1990. Geographical variations in the seasonal heating cycle in northwest European shelf seas. Cont. Shelf Res. 10, 185–199.
Butman, B., Beardsley, R.C., 1987. Long-Term observations on the southern flank of Georges Bank. Part I: A Description of the seasonal cycle of currents, temperature, stratification, and wind stress. J. Phys. Ocean. 17, 367–384.
Cetina-Heredia, P., Roughan, M., van Sebille, E., Coleman, M.A., 2014. Long-term trends in the East Australian Current separation latitude and eddy driven transport. J. Geophys. Res.: Ocean. 119, 4351–4366.
Church, J.A., Freeland, H.J., Smith, R.L., 1986. Coastal-Trapped Waves on the East Australian Continental Shelf Part I: Propagation of Modes. J. Phys. Ocean. 16, 1929–1943.
Cresswell, G., 1994. Nutrient enrichment of the Sydney continental shelf. Mar. Freshw. Res. 45, 677–691.
Dai, A., Trenberth, K.E., 2002. Estimates of freshwater discharge from continents: latitudinal and seasonal variations. J. Hydrometeorol. 3, 660–687.
Davis, X.J., Weller, R.A., Bigorre, S., Plueddemann, A.J., 2013. Local oceanic response to atmospheric forcing in the Gulf Stream region. Deep-Sea Res. Part II: Top. Stud. Ocean. 91, 71–83.
Everett, J.D., Baird, M.E., Oke, P.R., Suthers, I.M., 2012. An avenue of eddies: Quantifying the biophysical properties of mesoscale eddies in the Tasman Sea. Geophys. Res. Lett. 39, L16608.
Everett, J.D., Baird, M.E., Roughan, M., Suthers, I.M., Doblin, M.A., 2014. Relative impact of seasonal and oceanographic drivers on surface chlorophyll a along a Western Boundary Current. Prog. Ocean. 120, 340–351.
Freeland, H.J., Boland, F.M., Church, J.A., Clarke, A.J., Forbes, A.M.G., Huyer, A., Smith, R.L., Thompson, R.O.R.Y., White, N.J., 1986. The Australian Coastal experiment: a search for coastal trapped waves. J. Phys. Ocean. 16, 1230–1249.
Gibbs, M.T., Middleton, J.H., Marchesiello, P., 1998. Baroclinic response of Sydney shelf waters to local wind and deep ocean forcing. J. Phys. Ocean. 28, 178–190.
Gill, A.E., 1982. Atmosphere-Ocean Dynamics, 1st ed. Academic Press, New York.
Godfrey, J.S., Cresswell, G., Golding, R., Pearce, A.F., T.J., 1980. The separation of the East Australian Current. J. Phys. Ocean. 10, 430–440.
Gong, D., Kohut, J.T., Glenn, S.M., 2010. Seasonal climatology of wind-driven circulation on the New Jersey Shelf. J. Geophys. Res.: Ocean. 115, C04006.
Griffin, D.A., Middleton, J.H., 1991. Local and remote wind forcing of New South Wales inner shelf currents and sea level. J. Phys. Ocean. 21, 304–322.
Hahn, S.D., Rochford, D.J., Godfrey, J.S., 1977. Long-term variability of oceanographic data at the Port Hacking 50-metre station. Aust. J. Mar. Freshw. Res. 28, 57–66.
Hamon, B.V., Godfrey, J.S., Greig, M.A., 1975. Relation between mean sea level, current and wind stress on the east coast of Australia. Aust. J. Mar. Freshw. Res. 26, 389–403.
Huyer, A., Smith, R.L., Stabeno, P.J., Church, J.A., White, N.J., 1988. Currents off southeastern Australia: results from the Australian Coastal Experiment. Aust. J. Mar. Freshw. Res. 39, 245–288.
Nederlands Meteorologisch Instituut, 1949. Sea areas around Australia, Oceanographic and meteorological data. Koninklijk Nederlands Meteorologisch Instituut.
IOC, SCOR, IAPSO, 2010. The international thermodynamic equation of seawater – 2010: Calculations and use of thermodynamic properties.
Kohut, J.T., Glenn, S.M., Chant, R.J., 2004. Seasonal current variability on the New Jersey inner shelf. J. Geophys. Res.: Ocean. 109, C07S07.
Lentz, S.J., 2008. Seasonal variations in the circulation over the Middle Atlantic Bight continental shelf. J. Phys. Ocean. 38, 1486–1500.
Li, Y., He, R., McGillicuddy Jr, D.J., 2014. Seasonal and interannual variability in Gulf of Maine hydrodynamics: 2002–2011. Deep. Sea Res. Part II: Top. Stud. Ocean. 103, 210–222.
Liu, Y., Weisberg, R.H., 2012. Seasonal variability on the West Florida Shelf. Prog. Ocean. 104, 80–98.
Malcolm, H.A., Davies, P.L., Jordan, A., Smith, S.D.A., 2011. Variation in sea temperature and the East Australian Current in the Solitary Islands region between 2001–2008. Deep. Sea Res. Part II: Top. Stud. Ocean. 58, 616–627.
Mantovanelli, A., Keating, S., Roughan, M., Wyatt, L., Schaeffer, A. In review. Eulerian and Langrangian characterization of two counter-rotating frontal eddies in a western boundary current. J. Geophy. Res. Oceans.
Mata, M.M., Wijffels, S.E., Church, J.A., Tomczak, M., 2006. Eddy shedding and energy conversions in the East Australian Current. J. Geophys. Res. C.: Ocean. 111, C09034.
McClean-Padman, J., Padman, L., 1991. Summer upwelling on the Sydney inner continental shelf: The relative roles of local wind forcing and mesoscale eddy encroachment. Cont. Shelf Res. 11, 321–345.
McDougall, T.J., Jackett, D.R., Millero, F.J., Pawlowicz, R., Barker, P., 2012. A global algorithm for estimating Absolute Salinity. Ocean. Sci. 8, 1123–1134.
Newell, B.S., 1966. Seasonal changes in the hydrological and biological environments off Port Hacking, Sydney. Aust. J. Mar. Freshw. Res. 17, 77–91.
Rennie, S.E., Largier, J.L., Lentz, S.J., 1999. Observations of a pulsed buoyancy current downstream of Chesapeake Bay. J. Geophys. Res. C.: Ocean. 104, 18227–18240.
Ridgway, K.R., Godfrey, J.S., 1997. Seasonal cycle of the East Australian Current. J. Geophys. Res.-Oceans 102, 22921–22936.
Rossi, V., Schaeffer, A., Wood, J., Galibert, G., Morris, B., Sudre, J., Roughan, M., Waite, A.M., 2014. Seasonality of sporadic physical processes driving temperature and nutrient high-frequency variability in the coastal ocean off southeast Australia. J. Geophys. Res.: Ocean. 119, 445–460.
Roughan, M., Middleton, J.H., 2002. A comparison of observed upwelling mechanisms off the east coast of Australia. Cont. Shelf Res. 22, 2551–2572.
Roughan, M., Middleton, J.H., 2004. On the East Australian Current: Variability, encroachment, and upwelling. J. Geophys. Res.-Oceans 109, 1–16.
Roughan, M., Morris, B., 2011. Using high-resolution ocean timeseries data to give context to long term hydrographic sampling off Port Hacking, NSW, Australia, OCEANS'11-MTS/IEEE. IEEE, Piscataway, NJ, Univted S., Kona, Hawaii, 1–4.
Roughan, M., Morris, B.D., Suthers, I.M., 2010, NSW-IMOS: An Integrated Marine Observing System for Southeastern Australia. IOP Conference Series: Earth and Environmental Science 11, 1-6.
Roughan, M., Schaeffer, A., Suthers, I.M., 2015. Sustained Ocean observing along the coast of southeastern Australia: NSW-IMOS 2007-2014, Coastal Ocean Observing Systems. Elsevier (Academic Press), San Diego CA, pp. 76–98.
Schaeffer, A., Roughan, M., Morris, B.D., 2013. Cross-shelf dynamics in a Western Boundary Current regime: Implications for upwelling. J. Phys. Ocean. 43, 1042–1059.
Schaeffer, A., Roughan, M., Morris, B.D., 2014a. CORRIGENDUM. J. Phys. Ocean. 44, 2812–2813.
Schaeffer, A., Roughan, M., Wood, J.E., 2014b. Observed bottom boundary layer transport and uplift on the continental shelf adjacent to a western boundary current. J. Geophys. Res.: Ocean. 119, 4922–4939.
Strub, P.T., Allen, J.S., Huyer, A., Smith, R.L., 1987. Seasonal cycle of currents, temperature, winds and sea level over the northeast Pacific continential shelf: 35°N to 48°N. J. Geophys. Res. 92, 1507–1526.
Thompson, P.A., Baird, M.E., Ingleton, T., Doblin, M.A., 2009. Long-term changes in temperate Australian coastal waters: implications for phytoplankton. Mar. Ecol. Prog. Ser. 394, 19.
Tranter, D.J., Carpenter, D.J., Leech, G.S., 1986. The coastal enrichment effect of the East Australian. Curr. eddy field. Deep. Sea Res. Part A. Ocean. Res. Pap. 33, 1705–1728.
Wood, J.E., Roughan, M., Tate, P.M., 2012. Finding a proxy for wind stress over the coastal ocean. Mar. Freshw. Res. 63, 528–544.